Structural-Acoustic Vibration Reduction Using Switched Shunt Piezoelectric Patches: A Finite Element Analysis

Walid Larbi, Jean-François Deü, Monica Ciminello, Roger Ohayon

Structural-Acoustic Vibration Reduction Using Switched Shunt Piezoelectric Patches: A Finite Element Analysis

Walid Larbi, Jean-François Deü
Structural Mechanics and Coupled Systems Laboratory, Conservatoire National des Arts et Métiers (Cnam), Case 353, 2 rue Conté 75003, Paris

Monica Ciminello
University of Naples Federico II, Aerospace Engineering Department, Via Claudio 23, 80125 Napoli, Italy

Roger Ohayon
Structural Mechanics and Coupled Systems Laboratory, Conservatoire National des Arts et Métiers (Cnam), Case 353, 2 rue Conté 75003, Paris

In this paper, we present a finite element formulation for vibration reduction in structural-acoustic systems using passive or semipassive shunt techniques. The coupled system consists of an elastic structure (with surface-mounted piezoelectric patches) filled with an inviscid linear acoustic fluid. An appropriate finite element formulation is de-rived. Numerical results for an elastic plate coupled to a parallelipedic air-filled interior acoustic cavity are presented, showing the performances of both the inductive shunt and the synchronized switch shunt techniques.

Keywords: vibration reduction, structural-acoustic, piezoelectric patches, switch, shunt, finite element method

1 Introduction

A considerable amount of research is actually devoted to the study and design of new noise reduction strategies to improve acoustic comfort. Noise reduction can be practically achieved using passive sound absorbing materials such as foams or fibrous materials [1]. These materials generally provide adequate absorption at medium and high frequencies but bulky in mass and volume in the low frequencies range where the absorption increases with the thickness of the absorber. For these reasons and despite a complexity of the design and the external power required, a new trend is to use active techniques to reduce noise and vibrations particularly in applications in which the lightness of the structure is a necessity. In this context, many research focused on control systems with piezoelectric patches, bonded or embedded in structural elements, and shunted in a specific electric circuit [2].

A finite element model to study the response of a piezoelectric smart structure for a cabin noise problem is presented in Ref. [3]. The active control system implemented was a negative feedback. In Ref. [4], a methodology based on the impedance technique to synthesize a predesignated acoustic response from a structure driven by multiple piezoelectric transducer (PZT) patches is presented. The influences of the PZT mass and stiffness on the acoustic radiation of the host structure are investigated for vibroacoustic control. Lefèvre and Gabbert [5] presented the theoretical background of a new finite element software tool for solving 3D electromechanical-acoustical field problems. Numerical investigations were performed using a modal reduction technique based on the uncoupled modes of the system. Another approach to the sound and vibration controls is to combine active and passive devices. Some works have dealt with this subject. Ro and Baz [6], for instance, presented a paper in which the sound radiation from a vibrating flat plate coupled with an acoustic cavity is controlled using a single piezoelectric patch with an active control and passive constrained layer damping treatments. A finite element model is developed to study the fundamental phenomena governing the coupling between the dynamics of treated plates and acoustic cavity. The model is used to compute frequencies, mode shapes, and sound radiation for different control gains. Close agreements are obtained between theoretical predictions and experimental measurements. An attempt to control noise in a cabin is presented in the work of Gopinathan et al. [7]. Here, the authors have presented a finite element/boundary element formulation for modeling and analysis of the active-passive noise control system. The method considered for the numerical applications is a cubic cavity in which one of the walls is assumed to be a flexible panel, which radiates sound into the cavity. The piezoelectric patches are attached to the panel at a predetermined location. The sensor patches generate a voltage, then amplified, and put in feedback into the actuator using an optimal feedback controller. The interior of the flexible vibrating panel is covered with a sound absorber. A formulation to calculate the coupled response of composite shells with embedded piezoelectric layers and an enclosed acoustic fluid is presented in the paper of Kaljevic and Saravanos [8]. The methodology consists of three parts: the formulation for the electromechanical response of the piezoshell, the formulation of the 3D acoustic response of the enclosed fluid, and finally the combination of the previous formulation to calculate the coupled smart structure acoustic fluid response. They adopted a mixed field laminate theory with a layerwise approximation for the electric potential. A boundary element formulation is developed to calculate the

[1]Corresponding author

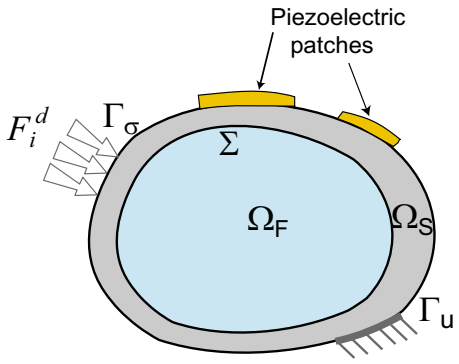

Fig. 1 Fluid/piezoelectric-structure coupled system

acoustic response of the enclosed fluid. A different approach to the noise reduction in sound radiating into a cavity is presented by Guyomar et al. [9]. The work deals with the semipassive approach in which the synchronized switch technique is implemented. The piezoceramics are continuously switched from the open circuit state to a specific electric network synchronously with the strain. The authors describe the experimental results with the analytical prediction. The experiment consists in exciting the plate via the loudspeaker and detects the noise level of the sound wave transmitted in the external environment. The measurement is made and compared in three cases: without control, with an inductive switched shunt, and with a voltage driving inductive switched shunt. The theoretical and experimental results are in good concordance; anyway, some discrepancies are observed, in particular, for the first mode. An attenuation of 15 dB on the transmitted wave pressure is obtained with the efforts of an amplification voltage driving source. Alternative active control procedure has also been derived [10], and experimental assessment of smart damping materials may be found in Ref. [11].

The present paper concerns a finite element formulation for vibration reduction in structural-acoustic systems using passive or semipassive shunt techniques. The coupled system consists of an elastic structure (with surface-mounted piezoelectric patch) filled with an inviscid, compressible, and barotropic fluid, gravity effect being neglected. Let us first recall that the general three-dimensional piezoelectric structure completely filled with acoustic fluid has already been discussed in Ref. [12]. On the other hand, an original procedure adapted to the vibrations of an elastic structure with shunted piezoelectric patches has been derived in Ref. [13]. The originality of the present paper is to extend the previous one to the structural acoustic case. Numerical results (in the low frequency domain) are analyzed, showing the performance of both the inductive shunt and the synchronized switch shunt techniques.

2 Finite Element Formulation of the Structural-Acoustic Problem With Piezoelectric Patches

First, we briefly recall the variational formulation of a fluid/piezoelectric-structure interaction problem in terms of structural mechanical displacement u_i, electric potential in the structure ψ, and fluid pressure p of the inviscid acoustic fluid (for more details, we refer the reader to Ref. [12]). Second, this coupled formulation is adapted to the general case of an elastic structure equipped with P piezoelectric patches (see Fig. 1), as done for structural vibrations in Ref. [13]. This modified formulation allows taking into account realistic electrical boundary conditions such as equipotentiality on patches electrodes and prescribed global charges. Finally, the resulting finite element formulation is applied to a structural acoustic problem with one piezoelectric patch connected to an *RL* series shunt circuit.

It should be noted that the standard indicial notations are adopted throughout the paper: Subscripts i, j, k, and l denote the 3D vectors and tensor components, and repeated subscripts imply summation. In addition, a comma indicates a partial derivative.

2.1 Variational Formulation of the Fluid/Structure/Piezoelectric-Patch Coupled System. We consider a piezoelectric structure occupying the domain Ω_S filled with an inviscid linear acoustic fluid occupying the domain Ω_F. We denote by Σ the fluid-structure interface and by n_i^S and n_i^F the unit normals external to Ω_S and Ω_F, respectively.

The structure is clamped on a part Γ_u and subjected (i) to a given surface force density F_i^d on the complementary part Γ_σ of its external boundary and (ii) to a pressure field p due to the presence of the fluid on its internal boundary Σ. The electric boundary conditions are defined by a prescribed electric potential ψ^d on Γ_ψ and a surface density of electric charge q^d on the remaining part Γ_D. Thus, the total structure boundary, denoted $\partial\Omega_S$, is such that $\partial\Omega_S=\Gamma_u\cup\Gamma_\sigma\cup\Sigma=\Gamma_D\cup\Gamma_\psi$ with $\Gamma_u\cap\Gamma_\sigma\cap\Sigma=\Gamma_\psi\cap\Gamma_D=\emptyset$.

The linearized deformation tensor is $\varepsilon_{ij}=\frac{1}{2}(u_{i,j}+u_{j,i})$, and the stress tensor is denoted by σ_{ij}. Concerning the electric field variables, D_i is the electric displacement verifying the electric charge equation for a dielectric medium $D_{i,i}=0$ in Ω_S and the electric boundary conditions $D_i n_i^S=-q^d$ on Γ_D; E_i denotes the electric field vector such that $E_i=-\psi_i$.

The linear piezoelectric constitutive equations write

$$\sigma_{ij}(u,\psi)=c_{ijkl}\varepsilon_{kl}(u)-e_{kij}E_k(\psi) \tag{1}$$

$$D_i(u,\psi)=e_{ikl}\varepsilon_{kl}(u)+\epsilon_{ik}E_k(\psi) \tag{2}$$

where c_{ijkl} denotes the elastic moduli at constant electric field, e_{kij} denotes the piezoelectric constants, and ϵ_{ik} denotes the dielectric permittivities at constant strain. Moreover, we denote by ρ_S the mass density of the structure.

Let us introduce the admissible spaces C_u and C_ψ of regular functions u_i and ψ defined in Ω_S. We then consider the following subspaces: $C_u^*=\{u_i\in C_u \,|\, u_i=0 \text{ on } \Gamma_u\}$, $C_\psi^d=\{\psi\in C_\psi \,|\, \psi=\psi^d \text{ on } \Gamma_\psi\}$, and $C_\psi^*=\{\psi\in C_\psi \,|\, \psi=0 \text{ on } \Gamma_\psi\}$.

The variational formulation, corresponding to the response of the piezoelectric structure subjected to the prescribed boundary conditions and to the pressure field p on the interface Σ, writes the following.

Find $u_i\in C_u^*$ and $\psi\in C_\psi^d$ such that

$$\int_{\Omega_S} c_{ijkl}\varepsilon_{kl}\delta\varepsilon_{ij}\,dv-\int_{\Omega_S} e_{kij}E_k\delta\varepsilon_{ij}\,dv+\rho_S\int_{\Omega_S}\frac{\partial^2 u_i}{\partial t^2}\delta u_i\,dv$$
$$=\int_{\Gamma_\sigma} F_i^d\delta u_i\,ds+\int_\Sigma p n_i^F\delta u_i\,ds \quad \forall\ \delta u_i\in C_u^* \tag{3}$$

where $\delta\varepsilon_{ij}=\frac{1}{2}(\delta u_{i,j}+\delta u_{j,i})$, ε_{kl} and E_k being the functions of u_i and ψ, and

$$\int_{\Omega_S} e_{ikl}\varepsilon_{kl}\delta E_i\,dv+\int_{\Omega_S}\epsilon_{ik}E_k\delta E_i\,dv=\int_{\Gamma_D} q^d\delta\psi\,ds \quad \forall\ \delta\psi\in C_\psi^* \tag{4}$$

where $\delta E_i=-\delta\psi_{,i}$, ε_{kl} and E_k being the functions of u_i and ψ.

This formulation must be completed by appropriate initial conditions.

We consider now the special case of an elastic structure (domain Ω_E) equipped with P piezoelectric patches and completely filled with an internal fluid (domain Ω_F). Each piezoelectric patch has the shape of a plate with its upper and lower surfaces covered with a very thin layer of conducting material to obtain electrodes. The pth patch ($p\in\{1,\cdots,P\}$) occupies a domain $\Omega^{(p)}$ such that $(\Omega_E,\Omega^{(1)},\cdots,\Omega^{(P)})$ is a partition of all the structure domain Ω_S.

A set of hypotheses that apply to a wide spectrum of practical applications is now formulated.

- The piezoelectric patches are thin, with a constant thickness denoted $h^{(p)}$ for the pth patch.
- The thickness of the electrodes is much smaller than $h^{(p)}$ and is thus neglected.
- The piezoelectric patches are polarized in their transverse direction (i.e., the direction normal to the electrodes).
- The electric field vector of components E_k is normal to the electrodes and uniform in the piezoelectric patch, so that for all $p \in \{1, \cdots, P\}$:

$$E_k = -\frac{V^{(p)}}{h^{(p)}} n_k \quad \text{in} \quad \Omega^{(p)} \tag{5}$$

where $V^{(p)} = \psi_+^{(p)} - \psi_-^{(p)}$ is the potential difference between the upper and the lower electrode surfaces of the pth patch, which is constant over $\Omega^{(p)}$, and n_k is the kth component of the normal unit vector to the surface of the electrodes.

Under those assumptions and by considering successively each of the $P+2$ subdomains $(\Omega_F, \Omega_E, \Omega^{(1)}, \ldots, \Omega^{(P)})$, the variational formulation of the fluid/structure/piezoelectric-patch coupled system can be written in terms of the structural mechanical displacement u_i, the electric potential difference $V^{(p)}$ constant in each piezoelectric patch, and the fluid pressure p:

- Mechanical equation

$$\begin{aligned} &\int_{\Omega_S} c_{ijkl}\varepsilon_{kl}\delta\varepsilon_{ij}\mathrm{d}v + \sum_{p=1}^{P} \frac{V^{(p)}}{h^{(p)}} \int_{\Omega^{(p)}} e_{kij} n_k \delta\varepsilon_{ij}\mathrm{d}\Omega \\ &\quad + \rho_S \int_{\Omega_S} \frac{\partial^2 u_i}{\partial t^2}\delta u_i \mathrm{d}v - \int_{\Sigma} p n_i^F \delta u_i \mathrm{d}s \\ &= \int_{\Gamma_\sigma} F_i^d \delta u_i \mathrm{d}s \quad \forall\ \delta u_i \in C_u^* \end{aligned} \tag{6}$$

- Electrical equation

$$\begin{aligned} &\sum_{p=1}^{P} \delta V^{(p)} C^{(p)} V^{(p)} - \sum_{p=1}^{P} \frac{\delta V^{(p)}}{h^{(p)}} \int_{\Omega^{(p)}} e_{ikl}\varepsilon_{kl} n_i \mathrm{d}\Omega \\ &= \sum_{p=1}^{P} \delta V^{(p)} Q^{(p)} \quad \forall\ \delta V^{(p)} \in \mathbb{R} \end{aligned} \tag{7}$$

  where $C^{(p)} = \epsilon_{33} S^{(p)} / h^{(p)}$ defines the capacitance of the pth piezoelectric patch ($S^{(p)}$ being the area of the patch and $\epsilon_{33} = \epsilon_{ik} n_i n_k$ being the piezoelectric material permittivity in the direction normal to the electrodes), and $Q^{(p)}$ is the global charge in one of the electrodes (see Ref. [13]).
- Acoustic equation

$$\begin{aligned} &\frac{1}{\rho_F}\int_{\Omega_F} p_{,i}\delta p_{,i}\mathrm{d}v + \frac{1}{\rho_F c_F^2}\int_{\Omega_F} \frac{\partial^2 p}{\partial t^2}\delta p \mathrm{d}v + \int_{\Sigma} \frac{\partial^2 u_i}{\partial t^2} n_i^F \delta p \mathrm{d}s \\ &= 0 \quad \forall\ \delta p \in C_p \end{aligned} \tag{8}$$

The first two equations are directly derived from Eqs. (3) and (4), using the procedure described in Ref. [13]. The last equation corresponds to the variational formulation of the Helmholtz equation in the acoustic cavity $p_{,ii} = (1/c_F^2)(\partial^2 p / \partial t^2)$ in Ω_F together with the boundary condition $p_{,i} n_i^F = -\rho_F (\partial^2 u_i / \partial t^2) n_i^F$ on Σ. This last relation expresses the continuity of the normal displacements of the inviscid fluid and the structure on Σ. c_F is the constant speed of sound in the fluid, and ρ_F is the mass density of the fluid. C_p is the admissible space of regular functions p defined in Ω_F.

Thus, the variational formulation of the fluid/structure/piezoelectric-patch coupled problem is written as follows: given (F^d, ψ^d, q^d), find $(u_i \in C_u^*,\ \psi \in C_\psi^d,$ and $p \in C_p)$ such that Eqs. (6)–(8) are satisfied. The formulation must be completed by appropriate initial conditions.

Remarks. This formulation, with only a couple of electric variables per patches, is well adapted to practical applications since (i) realistic electrical boundary conditions such that equipotentiality on the electrodes and prescribed global charges naturally appear, (ii) the global charge/voltage variables are intrinsically adapted to include any external electrical circuit into the electromechanical problem and to simulate shunted piezoelectric patches. We will not discuss in this paper the various symmetrization of the formulation using additional fluid variable such as fluid displacement potential, neither the regularization of the formulation for the limit static case, which necessitates the following constraint: $\int_{\Omega_F} p dv + \rho_F c_F^2 \int_{\partial\Omega_F} u_i n_i^F ds = 0$. This relation will be useful for the construction of a reduced order model of dynamic substructuring type. We refer to Refs. [12,14,15] for more details.

- Note that δu_i, $\delta\psi$, and δp are time independent and consequently, t is a parameter for the corresponding admissible spaces.

2.2 Finite Element Formulation of the Fluid/Structure/Piezoelectric-Patch Coupled System. Let us introduce $\mathbf{U}$ and $\mathbf{P}$ corresponding to the vectors of nodal values of u_i and p, respectively, and $\mathbf{Q} = (Q^{(1)} Q^{(2)} \cdots Q^{(P)})^T$ and $\mathbf{V} = (V^{(1)} V^{(2)} \cdots V^{(P)})^T$ the column vectors of electric charges and potential differences. The submatrices corresponding to the various linear and bilinear forms involved in Eqs. (6)–(8) are defined by

$$\int_{\Omega_S} c_{ijkl}\varepsilon_{kl}\delta\varepsilon_{ij} dv \Rightarrow \delta\mathbf{U}^T \mathbf{K}_u \mathbf{U} \tag{9a}$$

$$\int_{\Omega_S} \rho_S u_i \delta u_i \mathrm{d}v \Rightarrow \delta\mathbf{U}^T \mathbf{M}_u \mathbf{U} \tag{9b}$$

$$\sum_{p=1}^{P} \frac{V^{(p)}}{h^{(p)}} \int_{\Omega^{(p)}} e_{kij} n_k \delta\varepsilon_{ij} \mathrm{d}\Omega \Rightarrow \delta\mathbf{U}^T \mathbf{C}_{uV} \mathbf{V} \tag{9c}$$

$$\sum_{p=1}^{P} \frac{\delta V^{(p)}}{h^{(p)}} \int_{\Omega^{(p)}} e_{ikl}\varepsilon_{kl} n_i \mathrm{d}\Omega \Rightarrow \delta\mathbf{V}^T \mathbf{C}_{uV}^T \mathbf{U} \tag{9d}$$

$$\int_{\Sigma} p n_i^F \delta u_i ds \Rightarrow \delta\mathbf{U}^T \mathbf{C}_{up} \mathbf{P} \tag{9e}$$

$$\int_{\Sigma} u_i n_i^F \delta p ds \Rightarrow \delta\mathbf{P}^T \mathbf{C}_{up}^T \mathbf{U} \tag{9f}$$

$$\frac{1}{\rho_F}\int_{\Omega_F} p_{,i}\delta p_{,i} dv \Rightarrow \delta\mathbf{P}^T \mathbf{K}_p \mathbf{P} \tag{9g}$$

$$\frac{1}{\rho_F c_F^2}\int_{\Omega_F} p\,\delta p dv \Rightarrow \delta\mathbf{P}^T \mathbf{M}_p \mathbf{P} \tag{9h}$$

$$\sum_{p=1}^{P} \delta V^{(p)} C^{(p)} V^{(p)} \Rightarrow \delta\mathbf{V}^T \mathbf{K}_V \mathbf{V} \tag{9i}$$

$$\int_{\Gamma_\sigma} F_i^d \delta u_i ds \Rightarrow \delta\mathbf{U}^T \mathbf{F} \tag{9j}$$

$$\sum_{p=1}^{P} \delta V^{(p)} Q^{(p)} \Rightarrow \delta \mathbf{V}^T \mathbf{Q} \tag{9k}$$

where $\mathbf{M}_u$ and $\mathbf{K}_u$ are the mass and stiffness matrices of the structure, $\mathbf{C}_{uV}$ is the electric-mechanical coupled stiffness matrix, $\mathbf{K}_V = \text{diag}(C^{(1)} C^{(2)} \cdots C^{(P)})$ is a diagonal matrix filled with the P capacitances of the piezoelectric patches, $\mathbf{M}_p$ and $\mathbf{K}_p$ are the mass and stiffness matrices of the fluid, $\mathbf{C}_{up}$ is the fluid-structure coupled matrix, and $\mathbf{F}$ is the applied mechanical force vector.

Thus, the variational equations (6)–(8) for the fluid/structure/piezoelectric-patch coupled problem can be written, in discretized form, as the following unsymmetric matrix system:

$$\begin{bmatrix} \mathbf{M}_u & \mathbf{0} & \mathbf{0} \\ \mathbf{0} & \mathbf{0} & \mathbf{0} \\ \mathbf{C}_{up}^T & \mathbf{0} & \mathbf{M}_p \end{bmatrix} \begin{bmatrix} \ddot{\mathbf{U}} \\ \ddot{\mathbf{V}} \\ \ddot{\mathbf{P}} \end{bmatrix} + \begin{bmatrix} \mathbf{K}_u & \mathbf{C}_{uV} & -\mathbf{C}_{up} \\ -\mathbf{C}_{uV}^T & \mathbf{K}_V & \mathbf{0} \\ \mathbf{0} & \mathbf{0} & \mathbf{K}_p \end{bmatrix} \begin{bmatrix} \mathbf{U} \\ \mathbf{V} \\ \mathbf{P} \end{bmatrix} = \begin{bmatrix} \mathbf{F} \\ \mathbf{Q} \\ \mathbf{0} \end{bmatrix} \tag{10}$$

with appropriate initial conditions.

Remarks. *Open circuit case* $\mathbf{Q}=\mathbf{0}$: Using the second row of Eq. (10), the degrees of freedom associated with the electric potential difference can be expressed in terms of structure displacements as

$$\mathbf{V} = \mathbf{K}_V^{-1} \mathbf{C}_{uV}^T \mathbf{U} \tag{11}$$

Thus, after substitution of $\mathbf{V}$ into Eq. (10), we get the following problem in terms of $\mathbf{U}$ and $\mathbf{P}$:

$$\begin{bmatrix} \mathbf{M}_u & \mathbf{0} \\ \mathbf{C}_{up}^T & \mathbf{M}_p \end{bmatrix} \begin{bmatrix} \ddot{\mathbf{U}} \\ \ddot{\mathbf{P}} \end{bmatrix} + \begin{bmatrix} \mathbf{K}_u + \mathbf{K}_A & -\mathbf{C}_{up} \\ \mathbf{0} & \mathbf{K}_p \end{bmatrix} \begin{bmatrix} \mathbf{U} \\ \mathbf{P} \end{bmatrix} = \begin{bmatrix} \mathbf{F} \\ \mathbf{0} \end{bmatrix} \tag{12}$$

where the "added-stiffness matrix" $\mathbf{K}_A$, which is due to the electromechanical coupling [16], is given by

$$\mathbf{K}_A = \mathbf{C}_{uV} \mathbf{K}_V^{-1} \mathbf{C}_{uV}^T \tag{13}$$

Note that $\mathbf{K}_V$ being a diagonal matrix, $\mathbf{K}_V^{-1}$ is easily computed. *Short circuit case* $\mathbf{V}=\mathbf{0}$: This case is obtained when the piezoelectric coupling constants are set to zero, i.e., $\mathbf{K}_A=\mathbf{0}$, and lead to the classical (u_i, p) fluid-structure system:

$$\begin{bmatrix} \mathbf{M}_u & \mathbf{0} \\ \mathbf{C}_{up}^T & \mathbf{M}_p \end{bmatrix} \begin{bmatrix} \ddot{\mathbf{U}} \\ \ddot{\mathbf{P}} \end{bmatrix} + \begin{bmatrix} \mathbf{K}_u & -\mathbf{C}_{up} \\ \mathbf{0} & \mathbf{K}_p \end{bmatrix} \begin{bmatrix} \mathbf{U} \\ \mathbf{P} \end{bmatrix} = \begin{bmatrix} \mathbf{F} \\ \mathbf{0} \end{bmatrix} \tag{14}$$

Electromechanical modal coupling factor: The open circuit and short circuit normal modes are harmonic solutions of Eqs. (12) and (14), respectively, with $\mathbf{F}=\mathbf{0}$. These natural frequencies are used to calculate the generalized electromechanical modal coupling factor, for the system nth mode, defined by Refs. [17,18]:

$$k_n = \sqrt{\frac{(\omega_n^{\text{OC}})^2 - (\omega_n^{\text{SC}})^2}{(\omega_n^{\text{SC}})^2}} \tag{15}$$

where ω_n^{OC} and ω_n^{SC}, respectively, are the open circuit and short circuit nth system natural frequencies (i.e., with all piezoelectric patches short circuited or open circuited). This parameter characterizes the energy exchanges between the mechanical structure and the piezoelectric patches.

2.3 Structural-Acoustic Problem With One Piezoelectric Patch Connected to *RL* Series Shunt Circuit. The above discretized formulation (Eq. (10)) can be used for a wide range of applications of mechanical structures coupled with acoustic domain and associated with piezoelectric patches. It is particularly adapted to the case where the piezoelectric patches are "shunted," that is to say connected to a passive electrical network [19]. In this case, neither $\mathbf{V}$ nor $\mathbf{Q}$ are prescribed by the electrical network, but the latter imposes only a relation between them. In the case of a resonant shunt connected to one patch and composed of a resistance R and an inductance L in series (Fig. 2), we have this additional relation between the electrical potential difference V and the electric charge Q:

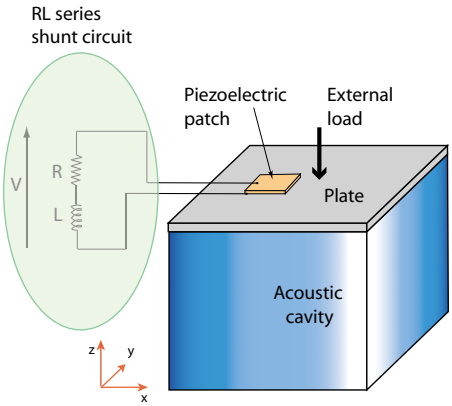

Fig. 2 Vibrating plate coupled with an acoustic cavity and connected to a *RL* shunt circuit

$$L\ddot{Q} + R\dot{Q} + V = 0 \tag{16}$$

Due to the direct piezoelectric effect, the piezoelectric patch converts a fraction of the mechanical energy of the vibrating structure into electrical energy, which can be dissipated through the resistive components of the *RL* circuit. It is well known that the damping effect due to this circuit is in maximum when the resonance circular frequency $1/\sqrt{LC}$ of the shunt circuit is tuned on the circular frequency of the structural-acoustic eigenmode to be controlled. The resistance R and the inductance L can be adjusted and properly chosen so as to maximize the damping effect (see Sec. 3.2).

Using the second row of Eq. (10) and noting that in the case of a single piezoelectric patch $\mathbf{K}_V=C$, the degrees of freedom associated with the electrical potential difference V can be expressed in terms of structural displacements $\mathbf{U}$ and electric charge Q as

$$V = \frac{1}{C} \mathbf{C}_{uV}^T \mathbf{U} + \frac{Q}{C} \tag{17}$$

Thus, after substitution of V into Eq. (16) and using Eq. (10), we get the following electromechanical-acoustic system:

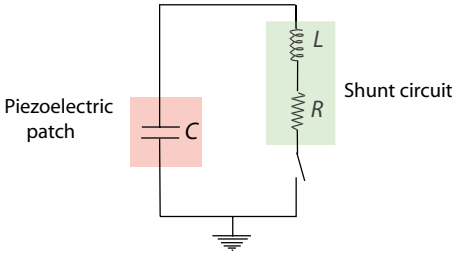

Fig. 3 PZT equivalent electrical circuit scheme within a switched shunt architecture

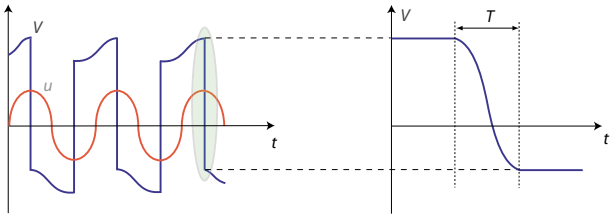

Fig. 4 Typical voltage and displacement waveforms for SSDI technique

$$\begin{bmatrix} \mathbf{M}_u & \mathbf{0} & \mathbf{0} \\ \mathbf{0} & L & \mathbf{0} \\ \mathbf{C}_{up}^T & \mathbf{0} & \mathbf{M}_p \end{bmatrix} \begin{bmatrix} \ddot{\mathbf{U}} \\ \ddot{Q} \\ \ddot{\mathbf{P}} \end{bmatrix} + \begin{bmatrix} \mathbf{0} & \mathbf{0} & \mathbf{0} \\ \mathbf{0} & R & \mathbf{0} \\ \mathbf{0} & \mathbf{0} & \mathbf{0} \end{bmatrix} \begin{bmatrix} \dot{\mathbf{U}} \\ \dot{Q} \\ \dot{\mathbf{P}} \end{bmatrix} + \begin{bmatrix} \mathbf{K}_u + \frac{1}{C}\mathbf{C}_{uV}\mathbf{C}_{uV}^T & \frac{1}{C}\mathbf{C}_{uV} & -\mathbf{C}_{up} \\ \frac{1}{C}\mathbf{C}_{uV}^T & \frac{1}{C} & \mathbf{0} \\ \mathbf{0} & \mathbf{0} & \mathbf{K}_p \end{bmatrix} \begin{bmatrix} \mathbf{U} \\ Q \\ \mathbf{P} \end{bmatrix} = \begin{bmatrix} \mathbf{F} \\ 0 \\ \mathbf{0} \end{bmatrix} \quad (18)$$

with appropriate initial conditions. Note that this $(\mathbf{U}, Q, \mathbf{P})$ formulation is well suited for switch shunting applications.

2.4 Application to Shunt Synchronized Switch Damping on Inductance. The synchronized switch damping on inductor (SSDI) technique is a semipassive approach that was developed to address the problem of structural vibration damping [18,20–22]. This particular nonlinear technique consists of adding a switching device in parallel with the piezoelectric patch. This device is composed of a switch, an inductance L, and a resistance R connected in series. Since the internal inductance and resistance of the piezoelectric material are very low in comparison to the inductance and resistance of the shunt circuit, the patch can be modeled by a capacitance C, as shown in Fig. 3. The switch is nearly always open, except when a displacement extremum occurs; at this moment, the switch is closed. The capacitance C of the piezoelectric patch and the inductance L thus constitute an electric oscillator. The switch is kept closed until the voltage V on the piezoelectric element has been inversed. It corresponds approximately to a time $T = \pi\sqrt{LC}$ equal to a half pseudoperiod of the electric shunt circuit. There is no particular value to which the inductance should be tuned, but it is chosen to get an inversion time T roughly between 10 and 50 times lower than the mechanical vibration period of interest [18,22]. When the switch is open and if no load is connected, the outgoing piezocurrent is null and then the voltage and the displacement vary proportionally. In Fig. 4, the typical voltage and displacement waveforms are shown with a zoom on the voltage inversion.

The synchronized switch damping technique provides more robustness if compared with the inductive shunt. The main advantages of this technique can be summarized with the following points:

- no need of large tuned inductor
- large band pass
- low sensitivity to environmental drifts
- good performance in transient regime
- no power amplifier and power supply needed
- no complex control logic
- simple and cheap hardware

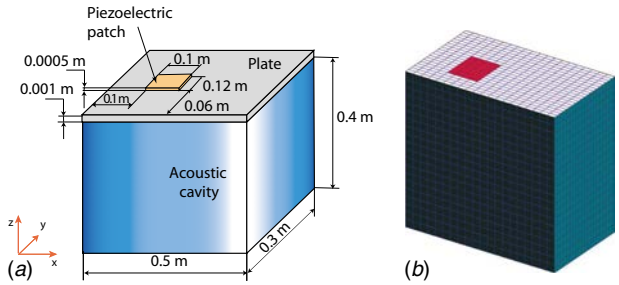

Fig. 5 Fluid/piezoelectric-structure coupled system: (*a*) geometrical data and (*b*) mesh (to scale)

Table 1 Mechanical data of piezoelectric PZT-5H material

	Material properties
c (GPa)	$c_{11}=c_{22}=126$, $c_{33}=117$ $c_{13}=c_{23}=84.1$, $c_{12}=79.5$ $c_{44}=c_{55}=23$, $c_{66}=23.3$
e (C m^{-2})	$e_{15}=e_{24}=17$, $e_{33}=23.3$ $e_{31}=e_{32}=-6.5$
ϵ (10^{-10} F m^{-1})	$\epsilon_{11}=\epsilon_{22}=150.3$, $\epsilon_{33}=130$
ρ (kg m^{-3})	7500

3 Numerical Examples

We present in this section the analysis of an interior damped structural-acoustic systems using (i) an inductive shunt and (ii) a synchronized switch damping technique, according to the finite element formulation described in Sec. 2. First, the modal analysis of the electromechanical-acoustic problem is presented. Then, the inductive shunt and switched techniques are compared in terms of attenuation of vibration and sound pressure level.

We consider a 3D acoustic cavity of size $A=0.5$ m, $B=0.3$ m, and $C=0.4$ m along the directions x, y, and z, respectively. The cavity is completely filled with air (density$=1.225$ kg/m^3; speed of sound$=340$ m/s). The cavity walls are rigid except the top one, which is a flexible aluminum plate of thickness (1 mm) clamped at its edges. The density of the plate is 2700 kg/m^3, the Young modulus is 72 GPa, and the Poisson ratio is 0.35. On the top surface of the plate, a PZT patch is bonded, whose in plane dimensions are 0.12×0.10 m^2 along x and y and 0.5 mm thick (see Fig. 5). The mechanical characteristics of the piezoelectric material (PZT-5H), related to the constitutive relations (1) and (2), are given in Table 1.

Concerning the finite element discretization, we have used, for the structural part, 400 four-node membrane-shear-bending plate elements (based on the first-order shear deformation theory) with five degrees of freedom per node and a selective reduced integration on the transverse shear. The portion of the plate covered by

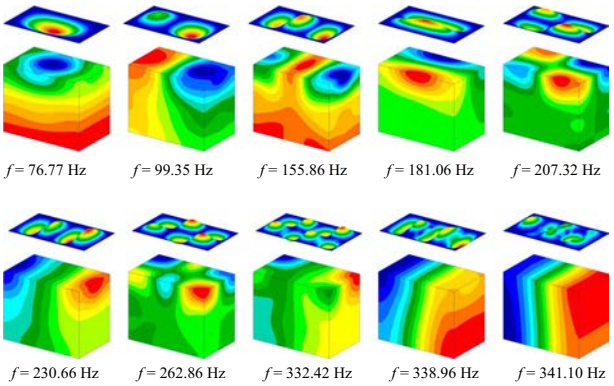

Fig. 6 Fluid-structure coupled modes: fluid pressure level and plate total displacement

Table 2 Computed frequencies (Hz) of the structural-acoustic coupled system

Fluid in a rigid cavity	Structure without fluid	Coupled problem	Type of coupled mode[a]
340.35	69.27	76.77	S
425.44	100.14	99.35	S
544.82	156.25	155.86	S
567.25	182.43	181.06	S
661.52	208.42	207.32	S
682.80	232.04	230.66	S
709.06	263.81	262.86	S
804.49	333.17	332.42	S
854.00	341.05	338.96	S
887.69	352.60	341.10	F

[a]S for structure mode and F for fluid mode.

the PZT patch and the patch itself has been modeled according to the first-order shear deformation laminate theory [23]. As discussed in Sec. 2, only one electrical degree of freedom is used to represent the electrical charge Q in the patch. The electromechanical coupling is obtained using the submatrix $\mathbf{C}_{uV}$ (see Eq. (9*c*) or Eq. (9*d*)).

The acoustic cavity is discretized using $20\times20\times20$ hexahedric elements with one degree of freedom per node corresponding to the acoustic pressure. The structural and acoustic meshes are compatible at the interface, and the fluid-structure coupling is realized through the $\mathbf{C}_{up}$ matrix (see Eq. (9*e*) or Eq. (9*f*)).

It is important to note that Eq. (12) (respectively, Eq. (14)) has been used to compute the fluid-structure normal modes in the open circuit case (Q=0) (respectively, short circuit case (V=0)) and Eq. (18) for the switch shunt application.

3.1 Modal Analysis of the Acoustic/Structure/ Piezoelectric-Patch Coupled Problem. Table 2 presents the eigenfrequencies in three following cases: (i) the 3D rigid acoustic cavity, (ii) the clamped plate with the patch short circuited, and (iii) the plate/acoustic-cavity coupled system in the short circuit case. The first nine coupled frequencies are associated with the first vibration modes of the structure (lower than 350 Hz), and the last coupled frequency corresponds to the first acoustic mode in the rigid cavity. This can be confirmed by comparing the mode shapes in case (iii) with those obtained in case (i) or case (ii), which are not shown here for the sake of brevity. Moreover, as expected, the natural frequencies of the coupled modes (structure dominated) are lower than those for the structure in vacuum (except for the first mode) due to the "added-mass effect" of the fluid.

For illustration purposes, Fig. 6 shows the deformed plate and the pressure field for the first ten vibration modes in the coupled case. The first eight modes are clearly dominated by the structural displacement, which induced the pressure level in the cavity. As shown in Table 2, the frequencies of coupled modes 9 and 10 are close to the first frequency of the acoustic mode in a rigid cavity and to the ninth mode of the structure in a vacuum. Thus, mode shapes (in terms of pressure and displacement) can be viewed as a combination of the shapes of the two associated uncoupled modes. We can also note that mode 9 is rather dominated by the structure displacement and mode 10 by the acoustic pressure.

3.2 Transient Analysis of the Acoustic/Structure/ Piezoelectric-Patch Coupled Problem. The plate is now excited by a normal sinusoidal force applied at its center and at the considered resonance frequency. The vibration output is detected at the center of the plate, where the displacement reaches a maximum, while the pressure is detected in the middle of the acoustic box. The responses in the open circuit case and in the inductive and synchronized switch cases are plotted and compared in time domain.

Table 3 Electrical parameters of the simulations

	Inductive shunt	Switched shunt
C (F)	956×10^{-9}	956×10^{-9}
L (H)	4.5	4.5×10^{-2}
R (Ω)	220	50

For the resonant shunt technique, the resistor and inductor in the electrical circuit are tuned to achieve a maximum energy dissipation from the mode to interest. Therefore, the optimal resistance and inductance for a series resonant shunt can be calculated by [19,18]

$$R^{\text{opt}} = \frac{\sqrt{2k_n^2}}{C\omega_n^{\text{SC}}(1+k_n^2)} \tag{19a}$$

$$L^{\text{opt}} = \frac{1}{C(\omega_n^{\text{SC}})^2(1+k_n^2)} \tag{19b}$$

where ω_n^{SC} is the short circuit natural frequency of the nth mode and k_n is the generalized electromechanical coupling coefficient

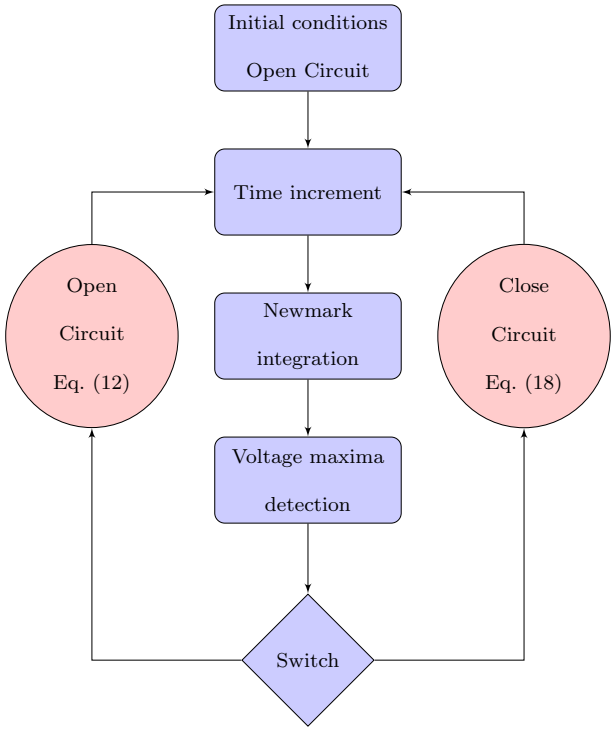

Fig. 7 Flowchart for the integration method used for the switch shunt system

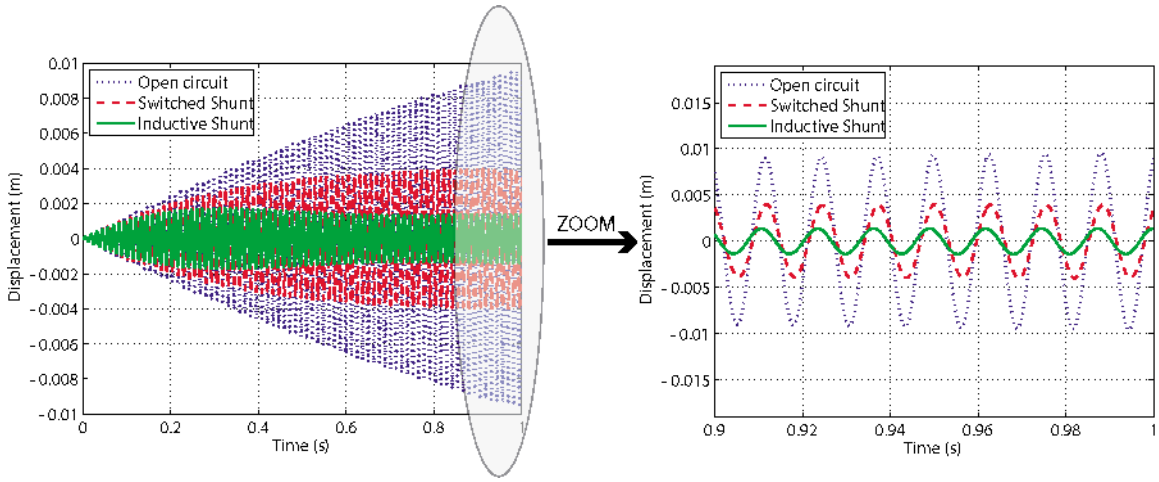

Fig. 8 Mechanical transverse displacement at the center of the plate under the first mode excitation frequency

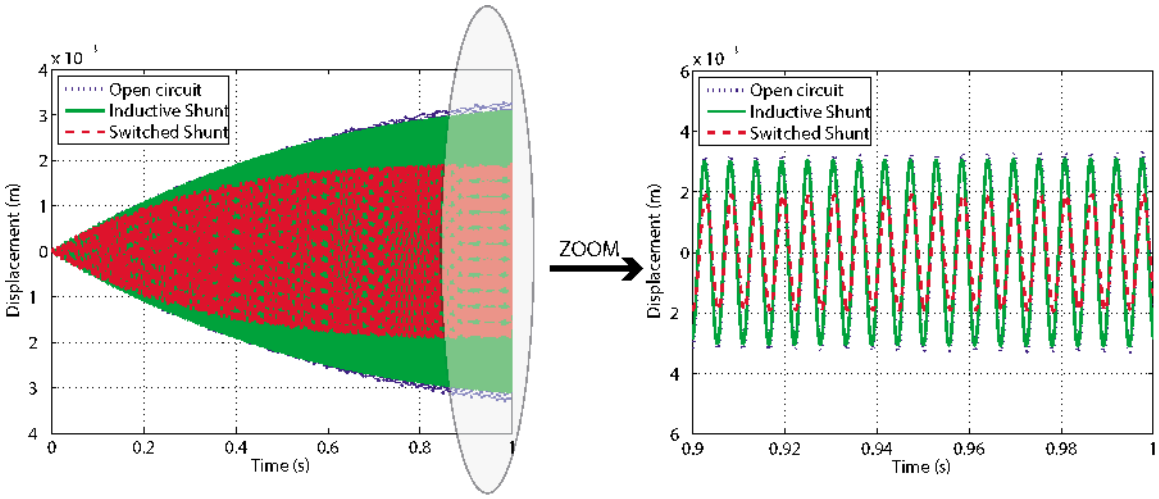

Fig. 9 Mechanical transverse displacement at the center of the plate under the fourth mode excitation frequency

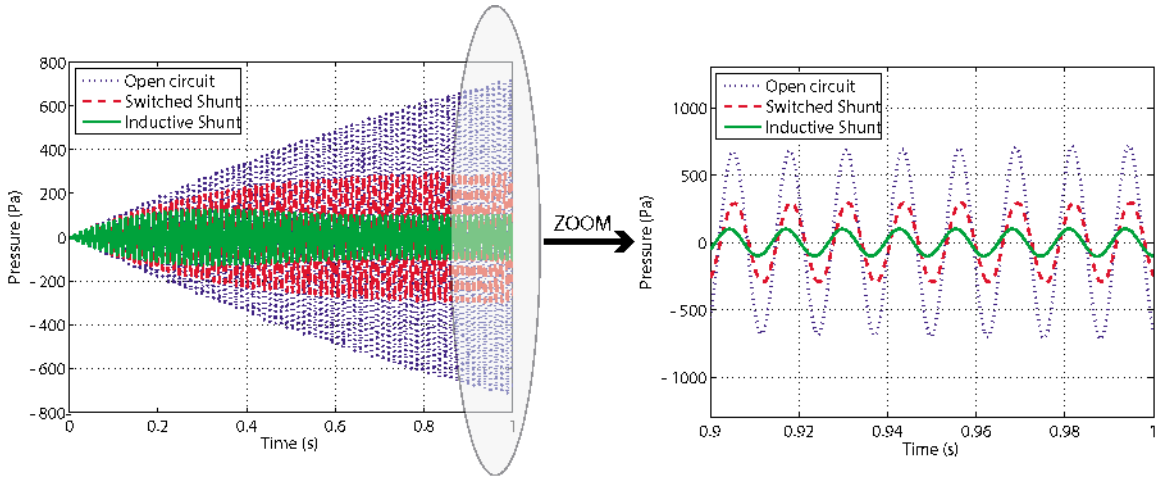

Fig. 10 Pressure level in the middle of the acoustic cavity under the first mode excitation frequency

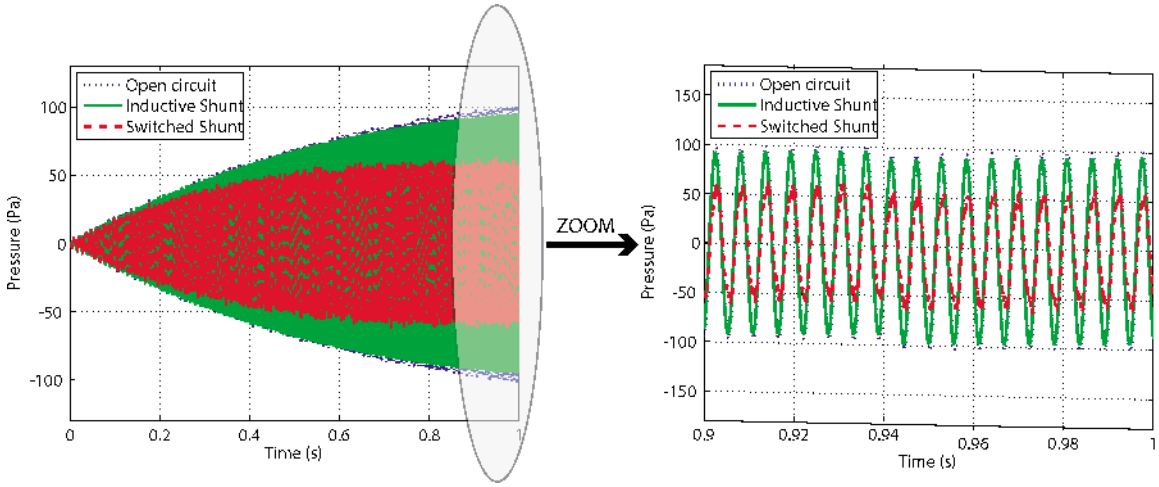

Fig. 11 Pressure level in the middle of the acoustic cavity under the fourth mode excitation frequency

given in Eq. (15).

Table 3 presents the electrical parameters adopted in the numerical simulation of the inductive shunt and the switched shunt devices. In the resonant shunt case, R and L are obtained using their optimal values (Eqs. (19*a*) and (19*b*)) associated with the first mode and with the electromechanical coupling coefficient $k_1=0.072$ ($\omega_1^{SC}=2\pi\times 76.77$ rad s^{-1} and $\omega_1^{OC}=2\pi\times 76.97$ rad s^{-1}). In the switched shunt case, the chosen inductance is $L=L^{opt}/100$, corresponding to a switching period $T=20$ times lower than the mechanical period of the first mode. Moreover, the resistance value is chosen more than four times lower than the optimal resistance of the passive shunt case. Here, this choice is somewhat arbitrary, but in practical applications, the optimal value can be obtained using a numerical optimization procedure.

Since the working principle of the switched shunt system is characterized by fast state variations, due to the electric circuit quick commutation times, the system behavior will suffer a continuous transient regime. Thus, a direct transient response analysis is needed. A computation in the time domain is performed using a direct implicit numerical scheme of the Newmark family algorithm. The output is computed assuming that the electrical circuit is closed or open (see Fig. 7).

In Figs. 8–11, the mechanical transverse displacement at the center of the plate and the sound pressure level in the middle of the acoustic cavity are plotted in three cases: (i) open circuit condition, (ii) inductive shunt, and (iii) switched shunt control. These time plots are obtained for two frequencies of the external sinusoidal excitation corresponding to the frequency of the first and fourth modes of the open-circuited coupled system.

Even if the steady state is not reached in the open circuit case, due to the fact that no mechanical damping has been introduced in the model, we can observe from these first results the effect of the attenuation performed by the two electrical systems.

The effects of the inductive shunt are evident just for the first mode (Figs. 8 and 10). The reason is due to the fact that the inductive shunt is tuned on the resonance frequency to be controlled, in the same way as the dynamic vibration absorber (or tuned-mass damper). So the electrical parameters should be changed according to the frequency of interest.

On the other hand, the switched shunt damping system shows wide band performances since the amplitude of both modes have been successfully reduced. Moreover, it is important to highlight that these results have been obtained with a very low inductor and a low resistor that give to the control system a higher thermal stability, very useful in aerospace applications. Finally, no external power supply has to be added to the system.

4 Conclusion

We have presented in this paper a finite element formulation of structural-acoustic problems with shunted piezoelectric patches. Two different kinds of vibration reduction techniques have been tested on an acoustic cavity coupled with an elastic plate and with a surface-mounted piezoelectric patch: the passive inductive shunt and the semipassive switched shunt. The numerical results show reduction in amplitudes achieved in a low frequency range with the switch control using only one piezoelectric patch and without any signal amplification. Moreover, attenuations are obtained, in the present example, without an optimization process to determine the best position of the patch. The results show the versatility of the proposed approach. Among future possible investigations, let us cite the problem of the experimental validation of the presented results, the analysis of more complex systems using appropriate reduced order models, and the optimization of the size and location of the piezoelectric patches in order to achieve high performances.

Acknowledgment

This research was partially supported by the European Community through the Marie Curie Research Training Network "A Computer Aided Engineering Approach to Smart Structures Design" under Contract No. MRTN-CT-2006-035559. The third author, Marie Curie Early Stage Researcher at CNAM/LMSSC during 2008/2009, is carrying a Ph.D. between University of Naples and CNAM.

References

[1] Larbi, W., Deü, J.-F., and Ohayon, R., 2006, "A New Finite Element Formulation for Internal Acoustic Problems With Dissipative Walls," Int. J. Numer. Methods Eng., **68**(3), pp. 381–399.
[2] Lesieutre, G. A., 2008, "Vibration Damping and Control Using Shunted Piezoelectric Materials," Shock Vib. Dig., **30**(3), pp. 187–195.
[3] Kim, J., Ko, B., Lee, J. K., and Cheong, C., 1999, "Finite Element Modelling of a Piezoelectric Smart Structure for the Cabin Noise Problem," Smart Mater. Struct., **8**(3), pp. 380–389.
[4] Lin, C., and Cheng, C., 2008, "Acoustic Response Synthesis Using Multiple Induced-Strain Actuators," ASME J. Vibr. Acoust., **130**(1), p. 011011.
[5] Lefèvre, J., and Gabbert, U., 2005, "Finite Element Modeling of Vibro-Acoustic Systems for Active Noise Reduction," Technische Mechanik, **25**(3–4), pp. 241–247.
[6] Ro, J., and Baz, A., 1999, "Control of Sound Radiation From a Plate Into an Acoustic Cavity Using Active Constrained Layer Damping," Smart Mater. Struct., **8**(3), pp. 292–300.
[7] Gopinathan, S., Varadan, V., and Varadan, V., 2000, "Finite Element/Boundary Element Simulation of Interior Noise Control Using Active-Passive Control Technique," Proc. SPIE, **3984**, pp. 22–32.

[8] Kaljevic, I., and Saravanos, D., 1997, "Steady State Response of Acoustic Cavities Bounded by Piezoelectric Composite Shell Structures," J. Sound Vib., **204**(3), pp. 459–476.
[9] Guyomar, D., Richard, T., and Richard, C., 2008, "Sound Wave Transmission Reduction Through a Plate Using a Piezoelectric Synchronized Switch Damping Technique," J. Intell. Mater. Syst. Struct., **19**(7), pp. 791–803.
[10] Balachandran, B., Sampath, A., and Park, J., 1996, "Active Control of Interior Noise in a Three-Dimensional Enclosure," Smart Mater. Struct., **5**(1), pp. 89–97.
[11] Ahmadian, M., Jeric, K., and Inman, D., 2001, "An Experimental Evaluation of Smart Damping Materials for Reducing Structural Noise and Vibrations," ASME J. Vibr. Acoust., **123**(4), pp. 533–536.
[12] Deü, J.-F., Larbi, W., and Ohayon, R., 2008, "Piezoelectric Structural Acoustic Problems: Symmetric Variational Formulations and Finite Element Results," Comput. Methods Appl. Mech. Eng., **197**(19–20), pp. 1715–1724.
[13] Thomas, O., Deü, J.-F., and Ducarne, J., 2009, "Vibrations of an Elastic Structure With Shunted Piezoelectric Patches: Efficient Finite Element Formulation and Electromechanical Coupling Coefficients," Int. J. Numer. Methods Eng., **80**(2), pp. 235–268.
[14] Morand, H.-P., and Ohayon, R., 1995, *Fluid-Structure Interaction*, Wiley, New York.
[15] Ohayon, R., and Soize, C., 1998, *Structural Acoustics and Vibration*, Academic, San Diego.
[16] Galucio, A., Deü, J.-F., and Ohayon, R., 2005, "A Fractional Derivative Viscoelastic Model for Hybrid Active-Passive Damping Treatments in Time Domain—Application to Sandwich Beams," J. Intell. Mater. Syst. Struct., **16**(1), pp. 33–45.
[17] 1988, ANSI/IEEE Standard 176-1987, IEEE Standard on Piezoelectricity.
[18] Corr, L., and Clark, W., 2002, "Comparison of Low-Frequency Piezoelectric Switching Shunt Techniques for Structural Damping," Smart Mater. Struct., **11**(3), pp. 370–376.
[19] Hagood, N., and von Flotow, A., 1991, "Damping of Structural Vibrations With Piezoelectric Materials and Passive Electrical Network," J. Sound Vib., **146**(2), pp. 243–268.
[20] Petit, L., Lefeuvre, E., Richard, C., and Guyomar, D., 2004, "A Broadband Semi Passive Piezoelectric Technique for Structural Damping," Proc. SPIE, **5386**, pp. 414–425.
[21] Badel, A., Sebald, G., Guyomar, D., Lallart, M., Lefeuvre, E., Richard, C., and Qui, J., 2006, "Piezoelectric Vibration Control by Synchronized Switching on Adaptive Voltage Sources: Towards Wideband Semi-Active Damping," J. Acoust. Soc. Am., **119**(5), pp. 2815–2825.
[22] Badel, A., Lagache, M., Guyomar, D., Lefeuvre, E., and Richard, C., 2007, "Finite Element and Simple Lumped Modeling for Flexural Nonlinear Semi-Passive Damping," J. Intell. Mater. Syst. Struct., **18**(7), pp. 727–742.
[23] Reddy, J., 2004, *Mechanics of Laminated Composite Plates and Shells: Theory and Analysis*, CRC, Boca Raton, FL.